

GAMMA-RAY BURSTER COUNTERPARTS: HST BLUE AND ULTRAVIOLET DATA

Bradley E. Schaefer

Department of Physics, Yale University, PO Box 208121, New Haven CT 06520-8121
schaefer@grb2.physics.yale.edu

Thomas L. Cline

Code 661, NASA/Goddard Space Flight Center, Greenbelt MD 20771
cline@lheavx.gsfc.nasa.gov

Kevin C. Hurley

Space Sciences Laboratory, University of California, Berkeley CA 94720
khurley@sunspot.ssl.berkeley.edu

John G. Laros

University of Arizona, Lunar and Planetary Laboratory, Tucson AZ 85721
jlaros@peewee.lpl.arizona.edu

ABSTRACT

The surest solution of the Gamma Ray Burst (GRB) mystery is to find an unambiguous low-energy quiescent counterpart. However, to date no reasonable candidates have been identified in the x-ray, optical, infrared, or radio ranges. The *Hubble Space Telescope (HST)* has now allowed for the first deep ultraviolet searches for quiescent counterparts. This paper reports on multiepoch ultraviolet searches of five GRB positions with HST. We found no sources with significant ultraviolet excesses, variability, parallax, or proper motion in any of the burst error regions. In particular, we see no sources similar to that proposed as a counterpart to the GRB970228. While this negative result is disappointing, it still has good utility for its strict limits on the no-host-galaxy problem in cosmological models of GRBs. For most cosmological models (with peak luminosity $6 \times 10^{50} \text{ erg} \cdot \text{s}^{-1}$), the absolute B magnitude of any possible host galaxy must be fainter than -15.5 to -17.4. These smallest boxes for some of the brightest bursts provide the most critical test, and our limits are a severe problem for all published cosmological burst models.

Subject headings: gamma rays: bursts

1. Introduction

Gamma Ray Bursts (GRBs) remain the biggest mystery in modern astrophysics. Much of the ‘blame’ for this lies in the fact that no unambiguous quiescent counterparts have been discovered. Historically, source classes first identified outside the optical band have had to await the detection of counterparts before their nature was determined. The need for the discovery of GRB counterparts has long been recognized, and this had led to deep searches down to the limits of modern technology in the x-ray, optical, infrared, and radio bands (see Schaefer 1994 for a review).

The launch and repair of the *Hubble Space Telescope (HST)* has opened up a new window in the ultraviolet (UV) for deep imaging in GRB error boxes. With the exception of the extreme ultraviolet (Hurley et al. 1993), no previous work has been published concerning searches at ultraviolet wavelengths. There are many reasons to expect that a counterpart might be most visible in the UV: (1) Bursters might be galactic objects with an accretion disk whose hot inner edge will emit copious amounts of UV light. (2) Bursters might be galactic neutron stars with a very hot surface temperature that will primarily emit

in the ultraviolet. (3) Bursters might be associated with quasars or active galactic nuclei which are characterized by UV excesses. All these reasonable possibilities suggest that we should examine this new window.

This paper reports on a search for UV counterparts to five GRBs with the HST. It is the fourth in a series of papers (with similar titles) which report results from large observational programs aimed at detecting burst counterparts. Previous papers reported deep near infrared limits for 7 GRBs and far infrared limits with the *IRAS* satellite for 23 GRBs (Schaefer et al. 1987), deep radio images with the *Very Large Array* telescope for 10 GRBs (Schaefer et al. 1989), and the examination of 32000 archival photographs for optical transients associated with 16 GRBs (Schaefer 1990). Additional work has been completed on deep optical searches for counterparts to 21 GRBs with 300 hours of integration time.

2. Observations

Gamma Ray Burst positional error regions range widely in size. Most bursts (for example, those detected by the *BATSE* detectors on the *Gamma Ray Observatory*) have typical positional uncertainties of several degrees, while triangulation between widely separated spacecraft can yield up to arc-minute sized boxes in a few optimal cases. Currently, only two classical GRB error regions have an area smaller than one square arc-minute. These are GRB790406 at 0.26 square arc-min and GRB790613 at 0.76 square arc-min. These sizes are to be compared to the fields-of-view of the two cameras on HST; 0.23'x0.23' for the FOC, and 2.5'x2.5' for the WFPC2. Few classical GRBs can be searched with HST if inefficient mosaics are to be avoided.

We were granted 7.0 hours of HST time in cycles 1 and 2 (proposal numbers 2378 and 3984) for two GRB with the FOC camera. The upheaval caused by the mirror aberration left us with the same amount of time, yet we only look ed at GRB790113 and the field of the OT1944 (Barat et al. 1984b, Schaefer et al. 1984, Schaefer 1990). For HST cycle 5 (after the aberrations were repaired and WFPC2 was installed), we were granted 16 orbits of time (proposal number 5839) for the four smallest classical GRB fields. A journal of observations is given in Table 1.

A basic problem in GRB counterpart searches is that we do not know *a priori* what a burster should look like. The many proposed burst models (Nemiroff 1994) have widely disparate properties for the associated counterparts. A general solution is to search for any unusual object within the positional error regions, the idea being that a sufficiently rare source is unlikely to appear inside a small box unless there is a causal connection. Thus,

counterpart searches become a statistical exercise in looking for anomalies. As most small boxes contain only faint sources, there are only a limited number of properties that can be efficiently examined. We can look for unusual colors (perhaps an ultraviolet excess), variability (perhaps caused by changing accretion or cooling), or motion across the sky (due to parallax or proper motion). A source in one of the small boxes that exhibits any of these properties might be sufficiently rare as to strongly argue for a causal connection with the burster.

Our observational strategy was optimized to detect these anomalies. We looked at multiple epochs (to test for variability) separated by a half year (to seek proper motion) at the times of quadrature (to be sensitive to parallax). We also looked in three filters so that we could construct our own color-color diagram from field objects. The UV filters we chose (F195W and F220W for the FOC images and F218W for the WFPC2 images) were selected based on their throughput for UV light and the minimization of any red leaks. These filters are broad band with FWHMs close to 40 nm and a central wavelength as given (in nm) in the filter name. The other two filters were the normal U filters (F342W for the FOC images and F336W for the WFPC2 images) and B filters (F430W for the FOC images and F439W for the WFPC2 images). The integration times were chosen to provide an equal signal-to-noise ratio for the three filters and an object with a Rayleigh-Jeans spectrum.

Full details on the detectors, filters, and calibrations are available in various documentation provided by the Space Telescope Science Institute (see especially Holtzman et al. 1995). Our data reduction has followed the standard pipeline processing recommended by Holtzman et al. (1995). In particular, we have used the PHOTFLAM data, the aperture corrections, the contamination corrections, and the charge-transfer-efficiency corrections. Our photometry likely has a systematic photometric uncertainty of a few hundredths of a magnitude (Holtzman et al. 1995). The median difference between measured magnitudes for the same star at the two epochs is 0.03 mag, while the standard deviation of these same measures is 0.08 mag. Thus, a systematic error of ~ 0.05 mag should be added in quadrature to all the statistical errors reported below.

3. Results

In all cases, the sources are not seen to move from epoch-to-epoch. The typical positional offset between epochs is under half a WFPC2 pixel, where one WFPC2 pixel is $0.10''$. (An object with a transverse velocity of $1000 \text{ km} \cdot \text{s}^{-1}$ will appear to move $0.05''$ in 180 days out to a distance of 2100 pc.) The number of stars in our color-color diagrams is small because only 6 stars were visible in the UV band, and 4 of these were saturated in the

B band. We found no case of significant photometric variability between epochs. Table 2 presents the photometry for sources inside the error boxes.

3.1. GRB790113

This GRB error box (Barat et al. 1984b) has a size of 78 square arc-minutes. The error region for the OT1944 (Schaefer et al. 1984, Schaefer 1990) is 0.05 square arc-minutes in size. This small region contains a faint M dwarf star which is suspected to have a time-variable ultraviolet excess (Schaefer 1986).

The FOC field-of-view was so small that only three stars appeared even in the B-band image. One of these is the OT1944 candidate star, while the other two were a pair of faint stars located roughly 15" to the east. With a ground based calibration of the brightness of the star pair, the brightness of the candidate is $B = 22.8 \pm 0.1$. Seven ground-based brightness measures for this source from 1983 to 1994 show B magnitudes ranging from 23.06 to 23.48 (with typical error of 0.11 mag) and one measure of 22.65 ± 0.3 . In the U-band, only the star pair was detected, while the candidate had a 5-sigma detection limit of ~ 24.0 for all epochs. In the UV-band, no source was ever detected at any epoch, with a typical 5-sigma threshold of ~ 22.1 mag. Geometric distortions and the lack of background stars prevented the co-adding of images from different epochs.

3.2. GRB790325

This GRB error box has a size of 2 square arc-minutes (Laros et al. 1985). The bright star 104 Herculis and the OT1946 (Hudec et al. 1987; Hudec, Peresty, & Motch 1990) are both nearby, but significantly outside the error box. No deep optical studies of this field have been published.

Over the whole field-of-view, the HST B-band images show 25 sources, the U-band images show 15 sources, while the UV-band images show only 1 source. Of the 25 sources, three are galaxies. The WFPC2 field-of-view completely covers the GRB box. Eight sources are inside the GRB error region, of which one is a galaxy (see Figure 1). The brightest source in the box is a G-type star that was saturated in the B-band, and had magnitude 14.50 ± 0.01 in the U-band, and 16.77 ± 0.01 in the UV-band. The only galaxy in the box has magnitudes $B = 21.98 \pm 0.05$ and $U = 23.23 \pm 0.37$. The limiting magnitudes for a 5-sigma detection are 23.0 in the B-band, 22.4 in the U-band, and 20.0 in the UV-band.

3.3. GRB790406

This burst has by far the smallest of all classical GRB error boxes (Laros et al. 1981). Previous optical studies have been published by Chevalier et al. (1981) and Motch et al. (1985).

Over the whole field-of-view, the HST B-band images show 10 sources, the U-band images show 9 sources, while the UV-band images show 2 sources (both near the limits of detection). Of these 10 sources, four are galaxies. None of these sources is inside or near the GRB error region. The limiting magnitudes for a 5-sigma detection are 22.8 in the B-band, 22.5 in the U-band, and 20.0 in the UV-band.

3.4. GRB790613

This burst has the second smallest of all classical GRB boxes (Barat et al. 1984a). Optical studies appear in Ricker, Vanderspek, & Ajhar (1986), Vrba, Hartmann, & Jennings (1995, VHJ), and Sokolov et al. (1995, SKZKB).

Over the whole field-of-view, the HST B-band images show 13 sources, the U-band images show 7 sources, while the UV-band images show 2 sources (both near the limits of detection). Of these 13 sources, five of them are galaxies. Three sources appear inside the GRB error box, and all three of these are galaxies. The first source (corresponding to object #63 in VHJ and galaxy 3 in SKZKB) has $B = 22.05 \pm 0.05$ and $U = 21.84 \pm 0.07$. The second galaxy in the GRB box (corresponding to object #71 of VHJ and galaxy 2 in SKZKB) has $B = 22.37 \pm 0.07$ and $U = 22.83 \pm 0.16$. The third galaxy (corresponding to object #57 of VHJ and object b in SKZKB) has $B = 22.33 \pm 0.06$ and $U = 22.09 \pm 0.15$. The limiting magnitudes for a 5-sigma detection are 23.2 in the B-band, 22.7 in the U-band, and 20.4 in the UV-band.

The GRB box is long and thin, and the extreme edges are outside the WFPC2 field-of-view. Close to 10% of the error box is not covered by the HST data; for this excluded portion, ground based images in the B- and R-bands do not show any sources that are bright enough to be expected to be visible. Thus, for galaxies, the limits on the brightest galaxy in the GRB790613 box are $B = 22.05 \pm 0.08$, $U = 21.84 \pm 0.07$, and $UV = 20.4$.

3.5. GRB920406

This GRB error box has a size of 2 square arc-minutes. No optical studies of this field have been published.

Over the whole field-of-view, the HST B-band and U-band images show 25 sources, while the UV-band images show only 1 source. Of these 25 sources, two are galaxies. The WFPC2 field-of-view misses the extreme tips of the GRB box, although 85% coverage is attained. Eight sources are inside the GRB error region, of which none is a galaxy (see Figure 2). The limiting magnitudes for a 5-sigma detection are 23.0 in the B-band, 22.6 in the U-band, and 19.5 in the UV-band.

4. Discussion

HST opens up a new window in the ultraviolet for GRB quiescent counterparts searches. We might expect to see such sources since bursters might contain hot accretion disks, hot neutron stars, or the blue cores of active galactic nuclei. Our search of five GRB error regions includes the four smallest classical GRB boxes. We have found no sources with any unusual property, including UV excess, variability, parallax, or proper motion. This lack of counterparts is disappointing. With these first UV searches, the entire accessible electromagnetic spectrum has now been examined for quiescent counterparts.

This lack of counterparts is nevertheless critical for several topics of recent interest. First, the GRB970228 has recently been associated with a fading x-ray transient which has been associated with an optical transient which has been associated with a faint point source superposed on an extended source (see IAU Circulars from numbers 6572 to 6631 for references). While each of these associations can be questioned and the various implications are currently unclear, the widely publicized interpretation is that the point source plus extended source is the quiescent counterpart. On the assumption that this identification is correct, we can examine whether similar counterparts are visible in our HST data. If the counterparts are similar to the GRB970228 candidate ($B=25.4$), then the expected brightness should scale as the GRB's peak flux. GRB970228 has a peak flux of roughly $1 \times 10^{-6} \text{ erg} \cdot \text{cm}^{-2} \cdot \text{s}^{-1}$, while the four classical GRBs have peak fluxes as listed in Table 4. The calculated B magnitudes for a counterpart like GRB970228 (see Table 3) were corrected for the galactic extinction as prescribed by Burstein & Heiles (1982). For comparison, Table 3 also lists our HST limits for extended sources and for extended sources associated with point sources. We see that any counterpart as proposed for GRB970228 should be easily detected in the boxes of GRB790406 and GRB790613. This could alternatively be viewed

as evidence against the identification of the GRB970228 candidate, evidence for a large spread in luminosity, or as evidence that both the extended and point source counterparts fade substantially on a time scale shorter than years.

Second, the presence of only very faint galaxies in these smallest of boxes is a strong challenge to most cosmological models of bursts. Let us take the peak luminosity to be $6 \times 10^{50} \text{ erg} \cdot \text{s}^{-1}$ (e.g., Fenimore et al. 1993) which is adopted for virtually all cosmological models due to the agreement with the LogN-LogP curves, the reported time dilation, and neutron star energetics. The distances can then be calculated for each burster based on their observed peak fluxes (see Table 4). The distance to the burster must be the same as the distance to the host galaxy. Then, the derived distance and our HST limit on the apparent magnitude of any extended source in the GRB region directly yield a limit on the absolute magnitude for the host galaxy. This limit must be corrected for the extinction through our galaxy, for which we have used the prescription in Burstein & Heiles (1982). The blue absorption is less than 0.3 mag in all cases, and this is confirmed by the lack of far infrared cirrus in the regions. In Table 4, we present our limits on the absolute magnitude for the host galaxies.

The host galaxies must therefore be fainter than absolute B magnitudes from -15.5 to -17.4. This is to be compared with the values for an L* galaxy of -21.0 and for a small irregular galaxy (like the SMC) of -16.2. Here, we have four-out-of-four GRBs that can have hosts no brighter than irregular galaxies. Such faint galaxies occupy the lowest $\sim 2\%$ of the galaxy luminosity function. The probability of getting such a result is $\sim 10^{-7}$ if the GRB hosts are drawn from a normal selection of galaxies. With four such limits, it is difficult to invoke a significant width to the luminosity function as an explanation.

Our result from HST by itself presents a no-host-galaxy dilemma for all cosmological models. Thus, now any acceptable cosmological model must explain the lack of host galaxies to deep limits. Only two potential solutions exist: (1) Bursts might be placed at such a great distance that the host is very faint. But to do this denies the observed dilation results, violates energy availability even for the annihilation of a whole neutron star, and forces a contrived evolution to explain the -1.5 slope of the bright portion of the LogN-LogP curve. (2) Bursts might be required to occur outside host galaxies. But then it is unclear why bursters exist only in intergalactic space, and most models require a galactic environment. We are not aware of any published cosmological model which has yet successfully solved the no-host-galaxy dilemma.

Support for this work has come under grants from the Space Telescope Science Institute (numbers 2378 and 5839) as well as NAG 5-1560 and JPL-958056.

REFERENCES

- Barat, C. et al. 1984a, ApJ, 280, 150; errata in 288, 833 and 299, 1079
- Barat, C. et al. 1984b, ApJ, 286, L5
- Burstein, D. & Heiles, C. 1982, AJ, 87, 1165
- Chevalier, C. et al. 1981, A&A, 100, L1
- Fenimore, E. E. et al. 1993, Nature, 366, 40
- Holtzman, J. A., Burrows, C. J., Casertano, S., Hester, J. J., Trauger, J. T., Watson, A. M., & Worthey, G. 1995, PASP, 107, 1065
- Hudec, R. et al. 1987, A&A, 175, 71
- Hudec, R., Peresty, R., & Motch, C. 1990, A&A, 235, 174
- Hurley, K., Li, P., Laros, J., Fishman, G., Kouveliotou, C., & Meegan, C. 1995, ApJ, 445, 348
- Laros, J. G. et al. 1981, ApJ, 245, L63
- Laros, J. G. et al. 1985, ApJ, 290, 728
- Motch, C., Pedersen, H., Ilovaisky, S. A., Chevalier, C., Hurley, K., & Pizzichini, G. 1985, A&A, 145, 201
- Nemiroff, R. J. 1994, Comments Astrophys., 17, 189
- Ricker, G. R., Vanderspek, R. K., & Ajhar, E. A. 1986, Adv. Space Sci., 6, 75
- Schaefer, B. E. 1986, Adv. Space Res., 6, 47
- Schaefer, B. E. 1990, ApJ, 364, 590
- Schaefer, B. E. 1994, in Gamma-Ray Bursts, eds G. J. Fishman, J. J. Brainerd, and K. Hurley (AIP: New York), p. 382
- Schaefer, B. E. et al. 1984, ApJ, 286, L1
- Schaefer, B. E. et al. 1987, ApJ, 313, 226
- Schaefer, B. E. et al. 1989, ApJ, 340, 455

Sokolov, V., Kurt, V. , Zharykov, S., Kopylov, A., & Berezin, A. 1995, Gamma Ray Bursts, eds C. Kouveliotou, M. Briggs, & G. Fishman (AIP: New York), p. 697 (SKZKB)

Vrba, F. J., Hartmann, D. H., & Jennings, M. C. 1995, ApJ, 446, 115 (VHJ)

Date	Detector	Target	Filters	Exposure
1991 Oct 3	FOC	GRB790113	UV, U	1782 s
1992 Mar 14	FOC	GRB790113	UV, U	1792 s
1992 Mar 20	FOC	GRB790113	UV, U, B	5000 s
1992 Sep 8	FOC	GRB790113	UV, U, B	2694 s
1995 Jul 8	WFPC2	GRB790613	UV, U, B	5000 s
1995 Sep 1	WFPC2	GRB790325	UV, U, B	4200 s
1995 Sep 6	WFPC2	GRB920406	UV, U, B	4400 s
1995 Oct 30	WFPC2	GRB790406	UV, U, B	4400 s
1995 Dec 29	WFPC2	GRB790613	UV, U, B	5000 s
1996 Feb 27	WFPC2	GRB790325	UV, U, B	4200 s
1996 Mar 4	WFPC2	GRB920406	UV, U, B	4400 s
1996 Apr 17	WFPC2	GRB790406	UV, U, B	4400 s
				13.1 hour

Table 1: Journal of HST GRB observations.

Region	Object Designation	B	U	UV	Comments
GRB790113	G	22.8	>24.0	>22.1	M star, variable in B?
GRB790325	A	(sat)	14.50	16.77	G star
	B	18.87	20.48	>20.0	
	C	20.61	>22.4	>20.0	
	D	21.98	23.23	>20.0	Galaxy
	E	18.37	19.23	>20.0	
	F	20.27	>22.4	>20.0	
	I	20.62	>22.4	>20.0	
	J	20.12	20.47	>20.0	
GRB790406	...	>22.8	>22.5	>20.0	Region is empty
GRB790613	VHJ#63	22.05	21.84	>20.4	Galaxy
	VHJ#71	22.37	22.83	>20.4	Galaxy
	VHJ#57	22.33	22.09	>20.4	Galaxy
GRB920406	A	(sat)	15.99	>19.5	
	B	18.95	19.83	>19.5	
	E	20.30	20.82	>19.5	
	I	16.41	17.37	>19.5	
	J	17.36	19.15	>19.5	
	L	17.45	18.24	>19.5	
	Y	20.52	21.29	>19.5	
	Z	19.32	19.69	>19.5	

Table 2: Sources inside error regions.

Region	Expected B for candidate like for GRB970228	B_{lim} for extended sources	B_{lim} for extended plus point sources
GRB790325	22.0	≥ 21.98	>23.0
GRB790406	21.2	> 22.8	>22.8
GRB790613	20.9	≥ 22.05	>23.2
GRB920406	23.2	> 23.0	>23.0

Table 3: Expected brightness of counterpart like proposed for GRB970228.

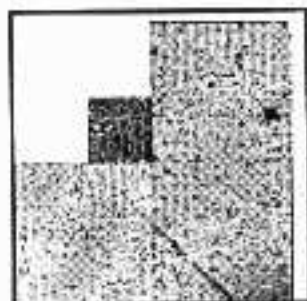
Region	Peak Flux ($erg \cdot cm^{-2} \cdot s^{-1}$)	Distance ^a (Mpc)	Galactic latitude	M_B^o for host galaxy
GRB790325	1.5×10^{-5}	580	22^o	≥ -17.2
GRB790406	2.4×10^{-5}	460	-61^o	> -15.5
GRB790613	3.2×10^{-5}	400	38^o	≥ -16.0
GRB920406	4.6×10^{-6}	1050	-28^o	> -17.4

Table 4: No-host-galaxy limits for the four classical GRB regions. ^a This assumes a peak luminosity of $6 \times 10^{50} erg \cdot s^{-1}$ as adopted by virtually all cosmological models of GRBs.

Fig. 1.— B mosaic for GRB790325. This WFPC2 image through the F439W filter shows no bright galaxies, as expected if bursters are in host galaxies. The only galaxy visible inside the error box is object D, at $B=21.98$. The diagonal streak is from the star 104 Her.

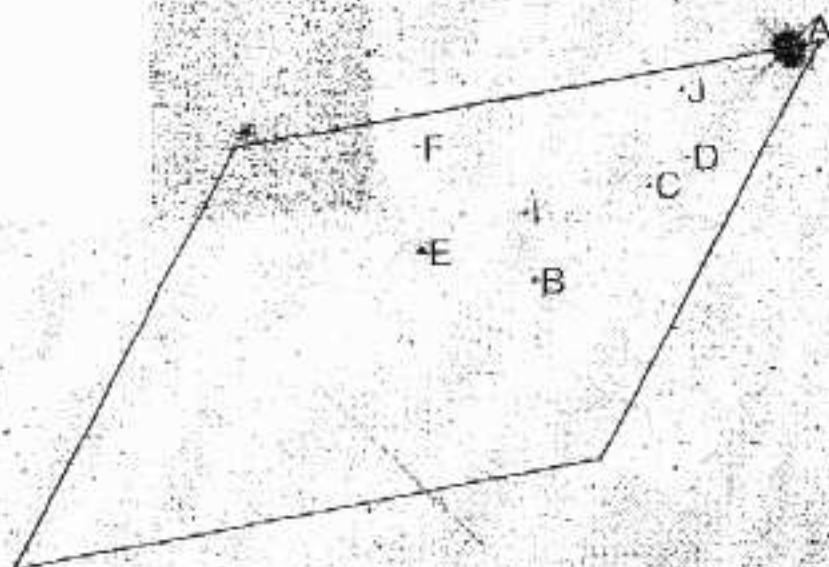
Fig. 2.— B mosaic of GRB920406. The error box extends to just outside the WFPC2 field of view, such that the observations cover 85% of the box. (Ground based images show no bright sources in the missing regions.) All objects inside the box are point sources, not galaxies.

g3be2.mos - G3BE2.MOS[1/1]
(IRAF)

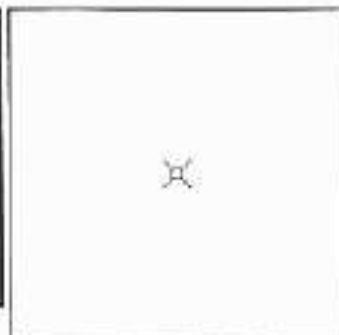
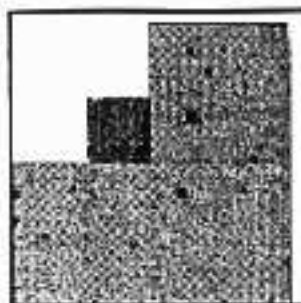


1660.0 1794.1 x

N ↙



g4be2.mos - G4BE2.MOS[1/1]
(IRAF)



1668.0 969.6 x

